Draft version January 11, 2017
Preprint typeset using LaTeX style emulateapj v. 03/07/07

arXiv:1701.02537v1 [astro-ph.SR] 10 Jan 2017

V773 CAS, QS AQL, AND BR IND: ECLIPSING BINARIES AS PARTS OF MULTIPLE SYSTEMS

P. Zasche[1] J. Juryšek[1,5] J. Nemravová[1] R. Uhlař[2] P. Svoboda[3] M. Wolf[1] K. Hoňková[4] M. Mašek[5] M. Prouza[5]
J. Čechura[6] D. Korčáková[1] M. Šlechta[6]

[1] Astronomical Institute, Charles University in Prague, Faculty of Mathematics and Physics, CZ-180 00, Praha 8, V Holešovičkách 2, Czech Republic
[2] Private Observatory, Pohoří 71, CZ-254 01, Jílové u Prahy, Czech Republic
[3] Private Observatory, Výpustky 5, CZ-614 00, Brno, Czech Republic
[4] Variable Star and Exoplanet Section of Czech Astronomical Society, Vsetínská 941/78, CZ-757 01, Valašské Meziříčí, Czech Republic
[5] Institute of Physics, The Czech Academy of Sciences, Na Slovance 1999/2, CZ-182 21, Praha, Czech Republic
[6] Astronomical Institute, The Czech Academy of Sciences, CZ-251 65, Ondřejov, Czech Republic

Draft version January 11, 2017

ABSTRACT

Eclipsing binaries still represent crucial objects for our understanding of the Universe. Especially those ones which are components of the multiple systems can help us solving the problem of their formation. The radial velocities together with the light curve analysis produced for the first time the precise physical parameters of the components of the multiple systems V773 Cas, QS Aql, and BR Ind. Their visual orbits were also analysed, resulted in slightly improved orbital elements. What is typical for all these systems is the fact that in all of them the most dominant source is the third distant component. The system V773 Cas consists of two similar G1-2V stars revolving on a circular orbit, while the more distant component is of A3V type. Additionally, the improved value of parallax was calculated to be of 17.6 mas. Analysis of QS Aql resulted in the following: inner eclipsing pair is composed of B6V and F1V stars, and the third component is of about B6 spectral type. The outer orbit has high eccentricity of about 0.95, and the observations near its upcoming periastron passage in between the years 2038-2040 are of high importance. Also the parallax of the system was derived to be of about 2.89 mas, moving the star much closer to the Sun than originally assumed. System BR Ind was found to be a quadruple star consisting of two eclipsing K dwarfs orbiting around each other with the period of 1.786 days, while the distant component is a single-lined spectroscopic binary with the orbital period of about 6 days. Both pairs are moving around each other on its 148 yr orbit.

Subject headings: stars: binaries: eclipsing – stars: binaries: spectroscopic – stars: fundamental parameters – stars: individual: V773 Cas, QS Aql, BR Ind

1. INTRODUCTION

Eclipsing binaries and multiple systems play a crucial role in our understanding of the Universe. The eclipsing binaries are being used for precise derivation of the stellar parameters such as radii, masses or luminosities. On the other hand, the multiple systems play an important role in our calibrations of models of star formation and evolution, because the presence of triple, quadruple, or even higher order systems can serve as a very sensitive indicator in these models and simulations. And finally, this distant component can play a crucial role during the evolution of the system, it offers the possibility to study the role of the so-called Kozai cycles with tidal friction (see e.g. Eggleton & Kiseleva-Eggleton 2001) or try to detect a slow precession of both inner and outer orbits.

Using the nowadays technique and large telescopes, automatic surveys and satellite observatories the borders of the astrophysical front-line research is still moving to the more distant and more faint targets. This is quite a logical process, but we have to be very careful when saying anything about completeness of our knowledge of bright and close systems. As was already stated in several recently published papers, also relatively bright targets among eclipsing binaries located within one hundred parsecs distance from the Sun can bring us quite new surprising results (see e.g. Mérand et al. 2011, or Nemravová et al. 2016).

Therefore, we focused our effort on three rather seldom-investigated systems (namely V773 Cas, QS Aql, and BR Ind) containing besides an inner eclipsing pair also a more distant third component detected via interferometry and having the orbital periods from several decades to hundreds of years (hence their ratio of periods is very large). Moreover, all of these stars show an Algol-like light curve and their spectroscopic as well as photometric study is still missing yet. As was already published earlier e.g. by Zasche et al. (2009) a list of such systems with eclipsing components among visual doubles, where both the inner and outer orbits are known is still very limited to only several dozens on the whole sky.

The statistics of the triple and multiple systems is still rather limited yet, but what can surely be said is that there is a lack of systems with higher-mass tertiary among the triple stars. This was shown e.g. by Tokovinin (2008) on spectroscopic triple stars or by Borkovits et al. (2016) on the Kepler eclipsing binaries. Only a small fraction of systems have the more massive tertiary than the eclipsing pair itself. And here comes our contribution to the topic.

2. THE DATA

The spectroscopy was obtained in two observatories. Most of the data points for these systems came from the Ondřejov observatory and its 2-meter telescope (resolution R $\sim$ 12500). Additionally, the data for BR Ind and some of the data for QS Aql were obtained with the FEROS instrument mounted on 2.2-meter MPG telescope located in La Silla Observatory in Chile (R $\sim$ 48000). The individual exposing times were chosen according to the quality of the particular night and specifications of the instrument to achieve the S/N ratio between several dozens to a few hundreds.

The original FEROS data were reduced using the standard routines. The final radial velocities (hereafter RV) used for the analysis were derived via a technique comparing both the direct and flipped profile of the spectral lines manually on the computer screen to achieve the best match, using program SPEFO (Horn et al. 1996, Škoda 1996) on several absorption lines in the measured spectral region (usually *Fe*, *Ca*, or *Si* lines). The derived radial velocities are given in Tables below in Appendix section.

The photometry for these three systems were collected during the time span from 2008 to 2016. However, some of the older data used only for the minima times were already published earlier, but the complete light curves (hereafter LC) are being published here for the first time. All of the data were obtained in the Johnson-Cousins photometric system Bessell (1990), particularly the system V773 Cas in BVR, while both the systems QS Aql and BR Ind in $BVRI$ filters.

Owing to the relatively high brightness of the targets, only rather small telescopes were used for these photometric observations. The system V773 Cas has been observed (by one of the authors: PS) with the 34-mm refractor at the private observatory in Brno, Czech Republic, using the SBIG ST-7XME CCD camera. The star QS Aql was monitored with the similar instrument at the private observatory (by one of the authors: RU) in Jílové u Prahy, Czech Republic, using a G2-0402 CCD camera. On the other hand, the only very southern star BR Ind was observed with the FRAM telescope (Prouza et al. 2010), installed and operated at the Pierre Auger Observatory at Malargüe, Argentina. For observations only a small Nikkor lens with 107 mm diameter and a CCD camera of G4-16000 type was used (which is mounted on 30-cm FRAM telescope itself). All the measurements were processed by the software C-MUNIPACK[1] which is based on aperture photometry and uses the standard DAOPHOT routines (Tody 1993).

3. THE ANALYSIS

The whole work is based on classical techniques of using the photometry and spectroscopy together with the analysis of the positional measurements of the visual double on the sky obtained during much longer time span (more than a century). Combining these methods together one can not only obtain the reliable orbital and stellar parameters, but also the structure of the system and its long-term evolution. The advantage is also the fact that having the complete information about the masses, inclinations, periods, etc. we can also fill in still rather incomplete statistics of the triple and quadruple systems, which is compared to models of formation of binaries and multiple systems (Tokovinin 2008).

At first, the visual orbit based on already published interferometric data was analysed. However, orbits of systems analysed within this study were published quite recently. Hence, our new re-calculations led to only slight improvements of the fits. The data were downloaded from the already published papers and the Washington Double Star Catalogue (hereafter WDS[2], Mason et al. 2001). The orbits were calculated following the paper Zasche & Wolf (2007), but the coverage of the orbits was usually not perfect and only parts of the long orbits are covered with data nowadays.

Both the photometry and spectroscopy were studied in the standard manner. The obtained photometric data and the radial velocities were analysed by the program Phoebe (Prša & Zwitter 2005), which is using the classical Wilson-Devinney algorithm (Wilson & Devinney (1971) and its later modifications) and allows us to fit the relevant parameters of the eclipsing components and their relative orbit. For the modelling, we used several assumptions. At first, the primary temperature was set to the value corresponding to the particular spectral type (see e.g. calibrations by Pecaut & Mamajek (2013) and the updated web site[3]). The limb-darkening coefficients were obtained through interpolation in tables by van Hamme (1993). The albedo coefficients A_i, and the gravity darkening coefficients g_i were fixed at their suggested values according to the temperatures of the components. As all studied eclipsing binaries are members of multiple systems third light from the remaining components was taken into account.

And finally, if we have the LC+RV solution and both the eclipsing binary masses are known, we can proceed to the combined analysis of the visual orbit together with the period changes of the eclipsing pair. The method itself was introduced in Zasche & Wolf (2007), and its usage was presented e.g. in Zasche et al. (2012), or Zasche et al. (2014). The most crucial for the whole analysis seems to be the quality of the input observations in both methods and the data coverage of the long orbit. This is usually problematic in these cases where the third-body orbit is too long and we have only small fraction of the orbit covered. On the other hand, if we have a good data coverage in both methods, we can even calculate independently the distance to the system.

4. V773 CAS

The first system in our sample of stars is the northern-hemisphere V773 Cas (= HIP 8115, HD 10543, V_{max} = 6.18 mag), an eclipsing binary discovered on the basis of Hipparcos data (Perryman & ESA 1997, and Kazarovets et al. 1999). However, many years before the discovery of its photometric variability was the star recognized as a visual binary. Its most recent orbital solution is that one published by Hartkopf & Mason (2009), who derived its period to be of about 193 yr, the orbital eccentricity of about 0.77, and the semimajor axis of about 0.9″. The spectral type was usually stated as A3V (Jaschek 1978) or A2V (Palmer et al. 1968). However, as noted by Cvetković & Ninković (2010), there arises a

[1] See http://c-munipack.sourceforge.net/

[2] http://ad.usno.navy.mil/wds/

[3] http://www.pas.rochester.edu/~emamajek/EEM_dwarf_UBVIJHK_colors_Teff.txt

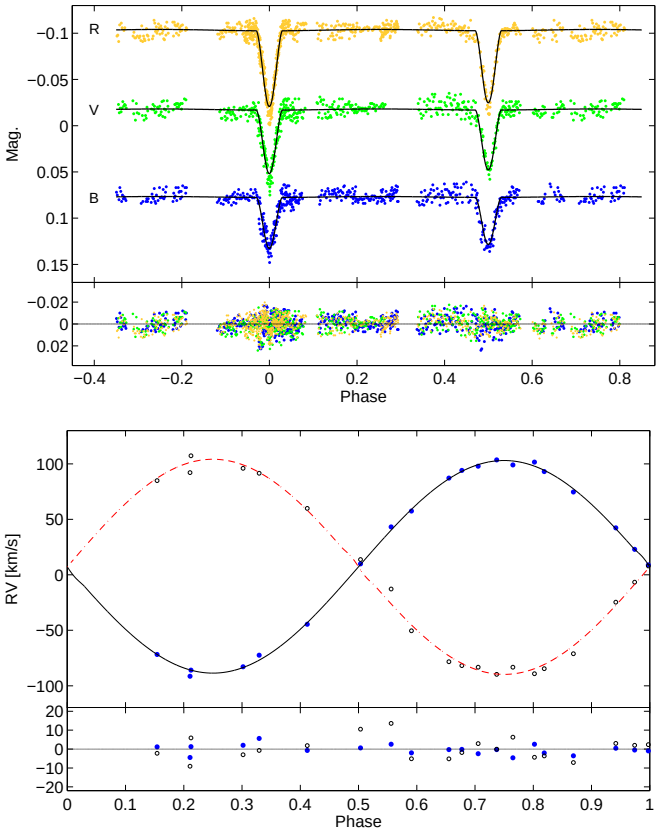

FIG. 1.— Light and radial velocity curve fits of V773 Cas based on the PHOEBE fitting.

large discrepancy between the astrophysical and dynamical total mass of the system. From its spectral types the total mass should be of about 3 $M_\odot$, while from the orbital solution arises that the $M_{dyn} = 11.9\ M_\odot$. This strange discrepancy originally led to our interest about the star.

First of all, we found out that for V773 Cas three new interferometric measurements were obtained since the last visual orbit calculation was published by Hartkopf & Mason (2009). We added these three data points and re-ran the fitting procedure again, resulted only in slightly different orbital solution. However, our solution would not be complete enough if we did not try to incorporate also the photometric monitoring and our results from the LC+RV analysis.

The primary temperature was kept fixed at a value of 5900 K, which resulted from our spectral estimations and also from the primary mass. The results of our LC+RV solution are shown in Figure 1, where one can see the light curve in BVR filters together with the RV curve based on the Ondřejov data. In total, there were obtained 20 spectrograms and 15 nights of photometry. The radial velocities were mostly derived from the *Ca* I and *Fe* I lines. The parameters of the least-squares fit are given in Table 1. The system is well-detached and both eclipsing components are probably of about G1-2V spectral type, hence should be considered as solar analogues. The spectral lines of both components seem to be very similar to each other, while some of the lines which remained at almost fixed position (at about 5 km·s^{-1}) seem to originate from the third distant body, whose movement is negligible over the time span of the observed

TABLE 1
THE PARAMETERS FROM THE LC+RV FITTING OF V773 CAS.

Parameter	Primary	Secondary	Tertiary
HJD_0	2448500.9209 ± 0.0003		–
P [d]	2.587332 ± 0.000002		–
a [$R_\odot$]	9.96 ± 0.06		–
v_γ [km/s]	7.11 ± 0.30		–
$q = M_2/M_1$	1.00 ± 0.05		–
i [deg]	84.7 ± 2.2		–
K [km/s]	97.1 ± 0.9	97.0 ± 1.6	–
T [K]	5900 (fixed)	5842 ±50	–
M [$M_\odot$]	0.99 ± 0.03	0.99 ± 0.04	–
R [$R_\odot$]	1.05 ± 0.05	1.05 ± 0.05	–
M_{bol} [mag]	4.55 ± 0.10	4.58 ± 0.10	–
L_B[%]	10.0 ± 0.9	9.5 ± 0.9	80.5 ± 0.9
L_V[%]	12.5 ± 0.7	12.1 ± 0.7	75.4 ± 0.6
L_R[%]	15.0 ± 0.6	14.6 ± 0.6	70.4 ± 0.5

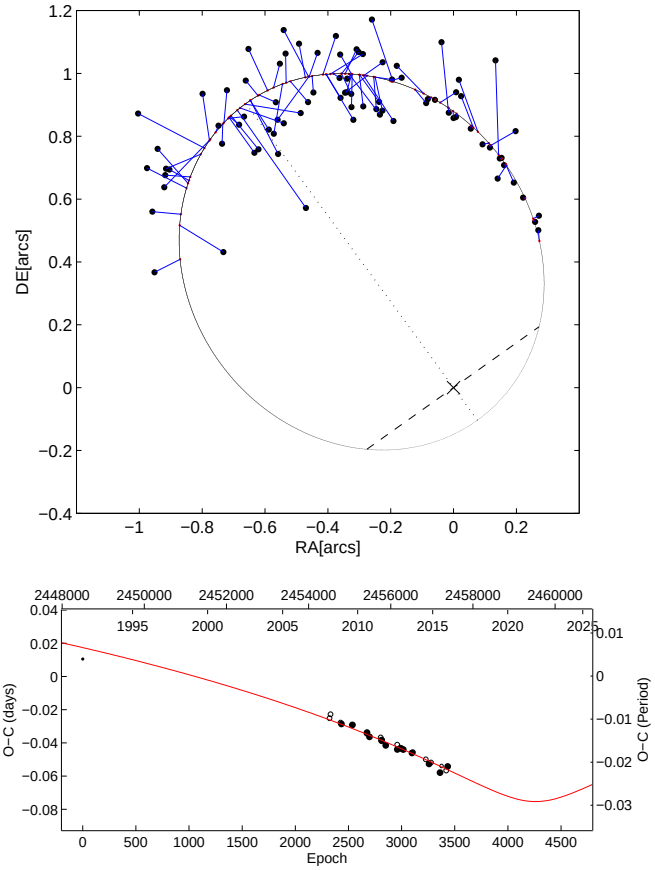

FIG. 2.— Upper plot: Orbit of V773 Cas on the sky. The individual observations are connected with their theoretical positions on the orbit, while the dotted line stands for the line of the apsides and the dashed line stands for the line of the nodes. Bottom plot: $O-C$ diagram of V773 Cas as resulted from our combined analysis of period changes together with the visual orbit. Best-fitting solution is plotted as a solid line, while the individual observations are denoted as filled (primary) and open (secondary) circles.

spectra. However, as one can see from the relatively high value of the third light as resulted from the LC solution, the third body is the brightest member of the system and it is probably responsible for the spectral classification of V773 Cas as A2-3 in the past.

The above-mentioned solution was derived using the PHOEBE code and the LC+RV fitting. However, we also tried a different approach to the problem. Us-

TABLE 2
Parameters of V773 Cas using Pyterpol.

Parameter	Primary	Secondary	Tertiary
T [K]	5933 ± 131	5693 ± 161	8522 ± 38
$v \sin i$ [km/s]	32.17 ± 2.32	49.10 ± 7.46	84.55 ± 1.42
L [%]	13.1 ± 0.8	11.1 ± 0.5	75.8 ± 0.6

TABLE 3
The orbital parameters of V773 Cas.

Parameter	Our solution	Hartkopf & Mason (2009)
p_3 [yr]	184.9 ± 2.7	193.17 ± 6.23
T_0 [yr]	2021.8 ± 2.1	2022.39 ± 0.78
e	0.794 ± 0.050	0.773 ± 0.016
a [arcsec]	0.911 ± 0.065	0.899 ± 0.012
i [deg]	133.3 ± 2.6	134.8 ± 3.8
Ω [deg]	125.4 ± 4.3	128.8 ± 4.6
ω [deg]	269.5 ± 8.5	270.2 ± 7.4

ing the available 20 spectrograms we applied the code Pyterpol[4](Nemravová et al. 2016). This program determines kinematic and radiative properties of binary components through comparison of observed spectra to synthetic ones obtained through interpolation in precalculated grids of synthetic spectra (de Laverny et al. 2012 and Palacios et al. 2010). Using this approach, we obtained the solution presented in Table 2. Such result is in very good agreement with the Phoebe solution presented above as well as with the observed magnitude difference between the two visual components (of about 1-2 mag from the WDS catalogue).

The linear ephemerides written in Table 1 are the best suitable elements for future prospective observations of V773 Cas in the upcoming years. However, these elements will change significantly due to the orbital motion of the eclipsing pair around a common barycenter with the third component. The most significant change of the orbital elements of the inner pair will take place near the periastron passage which will occur in 2021. We plotted the predicted period variation of V773 Cas eclipsing pair in the $O-C$ diagram in the Fig. 2. This diagram was constructed in agreement with the visual orbit of the double as resulted from our combined analysis. The orbit of the third component is given in Fig. 2 and the parameters of such a fit are given in Table 3. The list of minima times used for the analysis are given below in Appendix section.

The problem is that for achieving such a self-consistent solution, we cannot use the Hipparcos parallax as an input parameter. The spectral classification of about A3V for the third component comes not only from the already published papers, but also from our findings about the spectra (the lines indicate a spectral type of about A3), as well as from the photometric indices of the third body as resulted from the LC+RV solution. Hence, the total mass of the three components should be of about 4 $M_\odot$, which is in contradiction with the computed mass using the Hipparcos parallax $\pi_{HIP} = 11.77 \pm 0.67$ mas. Hence, the parallax needed for our combined solution to be self-consistent one needs the value of about $\pi_{new} = 17.6 \pm 1.5$ mas, but its uncertainty is still rather high because it is based only on a mass estimation. Such a situation is nothing novel, because there was already shown that the Hipparcos data sometimes produce spurious results for the close double stars, see e.g. Docobo et al. (2008).

[4] https://github.com/chrysante87/pyterpol/wiki

TABLE 4
The parameters from the LC+RV fitting of QS Aql.

Parameter	Primary	Secondary	Tertiary
HJD_0	2440443.5442 ± 0.0015		–
P [d]	2.5132987 ± 0.0000075		–
a [$R_\odot$]	13.78 ± 0.11		–
v_γ [km/s]	-16.13 ± 0.62		–
$q = M_2/M_1$	0.37 ± 0.02		–
i [deg]	83.6 ± 1.3		–
K [km/s]	73.98 ± 0.33	201.76 ± 2.09	–
T [K]	14500 (fixed)	7910 ± 78	–
M [$M_\odot$]	4.07 ± 0.09	1.49 ± 0.05	–
R [$R_\odot$]	4.08 ± 0.15	1.65 ± 0.20	–
M_{bol} [mag]	-2.31 ± 0.18	2.29 ± 0.14	–
L_B[%]	47.6 ± 2.9	1.4 ± 0.4	51.0 ± 3.1
L_V[%]	47.4 ± 1.2	2.0 ± 0.3	50.6 ± 1.4
L_R[%]	49.2 ± 3.4	2.3 ± 0.2	48.5 ± 3.5
L_I[%]	48.7 ± 2.3	2.7 ± 0.2	48.6 ± 2.5

5. QS AQL

Second eclipsing system analysed in the present study is QS Aql (=HIP 96840, HD 185936, $V_{max} = 6.01$ mag), which is the brightest one and also the most massive one among the studied systems. Jaschek (1978) classified its spectral type as B5V, while the others like Cannon & Pickering (1923) or Lu (1991) published its type as B3. Moreover, its variability was first detected by Millman (1928), but its eclipsing nature was confirmed by Guthnick (1931), who also gave its correct orbital period of about 2.5 days. Some 40 years later, Knipe (1971) discovered a rapid period change, which occurred at about 1964 (his suggestion) and was caused by the periastron passage in the wide orbit around the barycenter. The period change was so rapid that the eccentricity of the wide orbit must be very high. On the other hand, the first astrometric observations are more than 80 years old, but their accuracy is questionable due to small angular separation of the components. Many reliable speckle interferometric observations were obtained since 1976. The most recent orbital solution was computed by Docobo & Ling (2007), who derived its orbital period to be of 61.72 yr and surprisingly high eccentricity of about 0.966. The total mass of the system was estimated to be of about 20 $M_\odot$, but with rather high uncertainty. Mayer (2004) noted that the combined analysis of period changes together with the visual orbit is still problematic due to poor coverage of data by both methods.

We started the photometric monitoring of this interesting system in 2007, while the new spectroscopy was collected from 2012. Since the last calculation of its visual orbit by Docobo & Ling (2007) there was published one new observation of the visual double. The system is known as a single-lined spectroscopic binary, while the secondary as well as the tertiary component lines were not detected in the spectra. For the discussion about the individual RV solutions see below.

The light curve analysis was carried out using the data obtained in $BVRI$ filters in the Czech Republic in 2009 and 2010. The results are shown in Fig. 3, while the pa-

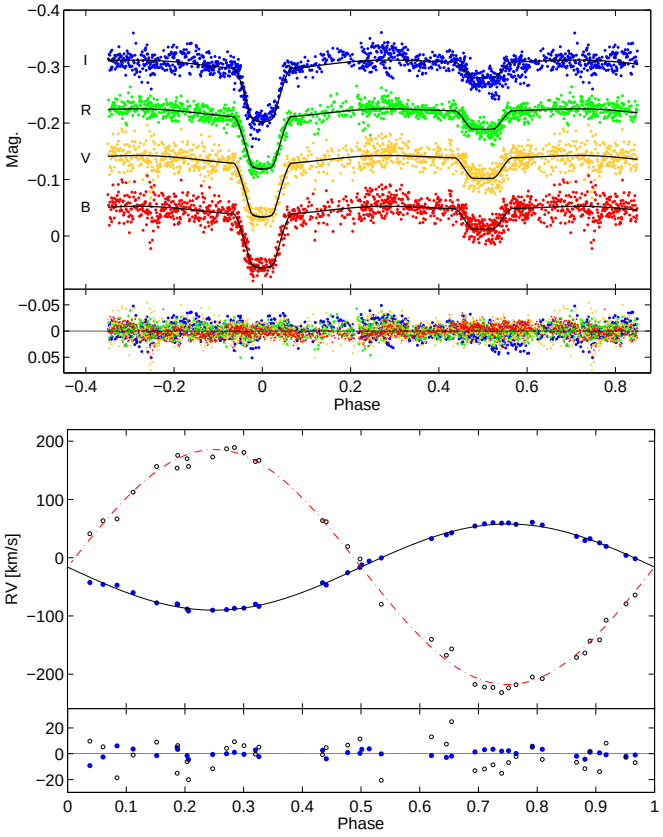

FIG. 3.— Light and radial velocity curve fits of QS Aql based on the PHOEBE fitting.

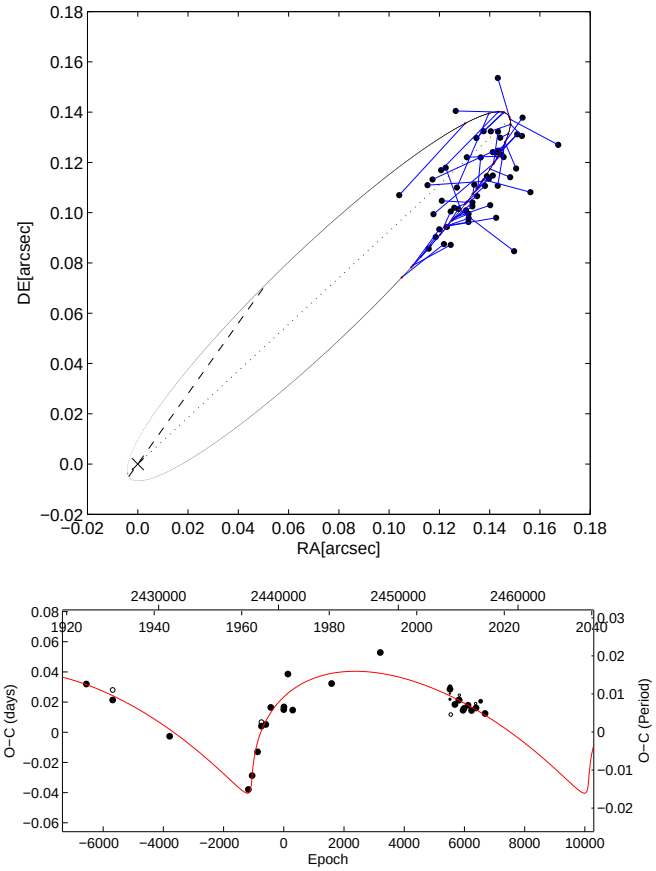

FIG. 4.— Orbit of QS Aql on the sky, and the $O-C$ diagram. See Fig. 2 for description.

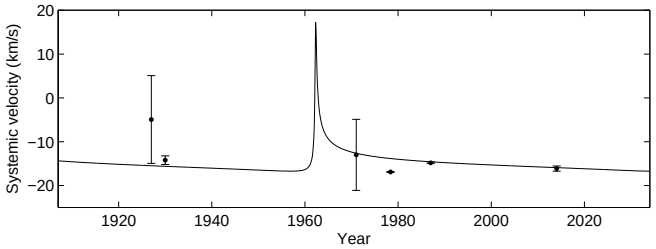

FIG. 5.— Gamma velocities of QS Aql as based on individual published RV solutions.

rameters corresponding to the best-fitting synthetic light curve are given in Table 4. In Fig. 3 you can also see some small variability on the residuals after subtraction of the light curve. However, these deviations are only caused by worse photometric conditions during some of the nights and our decision not to remove the outlying points on the light curves. The results of the RV fitting are shown in Fig. 3, where one can see that the secondary velocities were also derived, but are affected by much larger errors than primary ones.

As one can see from the parameters given in Table 4, the eclipsing components are rather different, but the most luminous one seems to be the third distant member. What is rather surprising is the fact that the amplitude of the RV variations for the primary component resulted in about 74 km/s, while the authors of the previous studies gave the K_1 value in between 40.8 km/s (Abt et al. 1990) and 58.4 km/s (Holmgren 1987). The other solutions gave also rather low values of K_1 about 47.3 km/s, see Hill (1931) and Lucy & Sweeney (1971). Explanation of this discrepancy probably comes from the fact that the lines are very broad and blended together with the third (dominant) component, which remains on almost the same position over the whole time interval. Thanks to this reason the lines are rather asymmetric and the previous authors probably measured the wide wings of the lines instead of the cores. If we measure the wings, the amplitude is really lower. However, thanks to the high dispersion FEROS spectra we were able to confidentially identify both the eclipsing components for the first time (hence SB1 becomes SB2) and derive the amplitude K_1 with higher conclusiveness.

If we tried to obtain a combined solution of the visual orbit plus the period variation of the eclipsing pair, we found out that the analysis is still rather problematic. For the trustworthy fit of the visual orbit only the data obtained since 1976 were taken into account. On the other hand, the older times of minima were also used because these define the rapid period change near the year 1960 quite well. For the results of our fitting see Fig. 4. The parameters of our solution are presented in Table 5.

As a by-product of the fitting we also plotted the gamma velocity changes in agreement with the third body orbit and plotted there also the individual gamma velocities as resulted from individual studies as published during the last century. Our result is shown in Fig. 5. Unfortunately, some individual systemic velocities are affected by large uncertainties and the predicted RV variation is rather flat during most of the p_3 period.

TABLE 5
THE PARAMETERS OF OUR COMBINED SOLUTION FOR QS AQL.

Parameter	Value
p_3 [yr]	77.0 ± 4.3
T_0 [yr]	1962.3 ± 2.3
e	0.947 ± 0.038
a [arcsec]	0.111 ± 0.045
i [deg]	61.2 ± 3.6
Ω [deg]	144.5 ± 5.1
ω [deg]	336.8 ± 4.7
M_3 [$M_\odot$]	4.04 ± 0.86
π [mas]	2.89 ± 0.55

However, a discussion of this combined solution is necessary. The presented final fits are still rather preliminary and especially the astrometry suffers from many deviating points. This is probably caused by rather large eccentricity and the inclined orbit. Several much more reliable observations would be very useful in the upcoming years. In the paper Heintze et al. (1989) the authors discussed the spectroscopic orbit by Holmgren (1987) and concluded that the third light should be of about 1.2 times larger than the combined light of the eclipsing pair. Their conclusion would imply tertiary mass 4.3 $M_\odot$ and spectral type of B5-6 V. However, this assumption is contradicted by the last interferometric observations, which indicate that both visual components are of similar brightness (i.e. the combined light from the eclipsing pair roughly the same as the third star), which is also in agreement with our new LC+RV solution. From this information we can derive that the third component is probably of about the same spectral type as the primary, i.e. B6V with the mass of about 4 $M_\odot$. Exactly the same result was obtained from our combined analysis of period changes and the visual orbit, see Table 5.

Thanks to the relatively well-derived amplitudes of both phenomena (semimajor axis for the visual orbit as well as the semiamplitude of the period variations in the $O-C$ diagram) we also tried to determine independently distance to the system. Quite interesting is the fact how the parallax of QS Aql has changed from the original Hipparcos value 1.98 ± 0.82 mas (Perryman & ESA 1997), while the new one was recalculated to 0.49 ± 0.62 mas (van Leeuwen 2007). On the other hand, Docobo & Andrade (2006) presented two different possible values of parallax based on two different methods and the Hipparcos parallax, namely 1.8 mas and 3.1 mas. No other parallax estimation has been found in the literature. However, from our solution there resulted that the parallax value have to be larger than the Hipparcos ones due to the amplitudes in both methods, of about 2.89 mas. The future space missions like GAIA (Perryman et al. 2001) would solve this problem, however the star is too bright and close to the bright limit of the satellite.

6. BR IND

The last system in our analysis is rather neglected and only seldom-investigated BR Ind (= HIP 104604, HD 201427, V_{max} = 7.07 mag). Its photometric variability was discovered on the basis of the Hipparcos data (Perryman & ESA 1997), giving the orbital period of 0.89277 days (a short note about its possible double value was also added there). Its spectral type F8V was published by Houk (1978), however it is not clear to which component this classification belongs. The star is also known as a visual double, having the time span of the positional observations of more than 100 yrs. The most recent orbital solution was published by Seymour et al. (2002), who derived the period of 167 yr, semimajor axis of 0.894″ and eccentricity of 0.521. However, since than five new observations were obtained and the orbit should be recalculated.

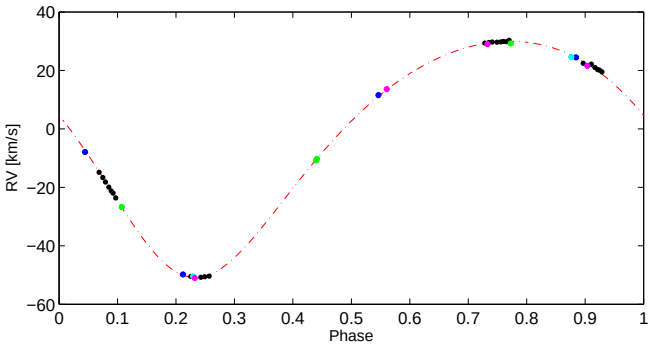

FIG. 6.— Radial velocity curve of the B pair of BR Ind as obtained from the FEROS data. The black dots stand for the data from fall 2013, blue ones are from fall 2014, green dots denote the data from spring 2015, the cyan ones are the observations coming from fall 2015, while the magenta ones are from spring 2016.

We collected the available photometry of BR Ind trying to find out which of the orbital periods is the correct one (0.89 or 1.78 days). However, the photometry from the surveys like ASAS (Pojmanski 1997) or Pi of the sky (Burd et al. 2005) were not able to distinguish between these two periods. Therefore, the photometry for BR Ind in $BVRI$ filters was obtained in 2014 and 2015 using the FRAM telescope. Thanks to these data we finally confirmed that the correct orbital period of the inner pair is really double, i.e. of about 1.786 days.

On the other hand, we also obtained the spectroscopy of BR Ind with the FEROS spectrograph in La Silla. However, after four nights (and obtaining 27 échelle spectra) of observations we were not able to detect the 1.8-days period on the most prominent lines. Instead, the lines follow some longer periodicity of several days. Hence, we applied for more observing time using the Tycho Brahe proposals for the 2.2-meter MPG telescope and the FEROS instrument again. During four consecutive seasons we obtained 14 more spectra of BR Ind leading finally to the solution.

The most prominent lines which were also used to derive the radial velocities were the Fe and Ca lines. These were analysed leading to the detection of a 6-days variation. Only much weaker lines were detected as the lines coming from the primary and secondary components of the eclipsing pair and following the 1.786-days variability. Hence, for the subsequent analysis we denoted the 6-days orbit as the "B" component, while the eclipsing pair is always designated as "A". The results of our RV fitting are plotted in Figs. 6 and 7. Resulting parameters of the pair B are given in Table 6. As one can see, the orbit is only slightly eccentric. Structure of BR Ind is plotted in Fig. 8.

The light curve fitting was carried out together with the radial velocity analysis in PHOEBE. The results are plotted in Fig. 7, while the parameters are given in Table 6. We can see that both components are very similar to

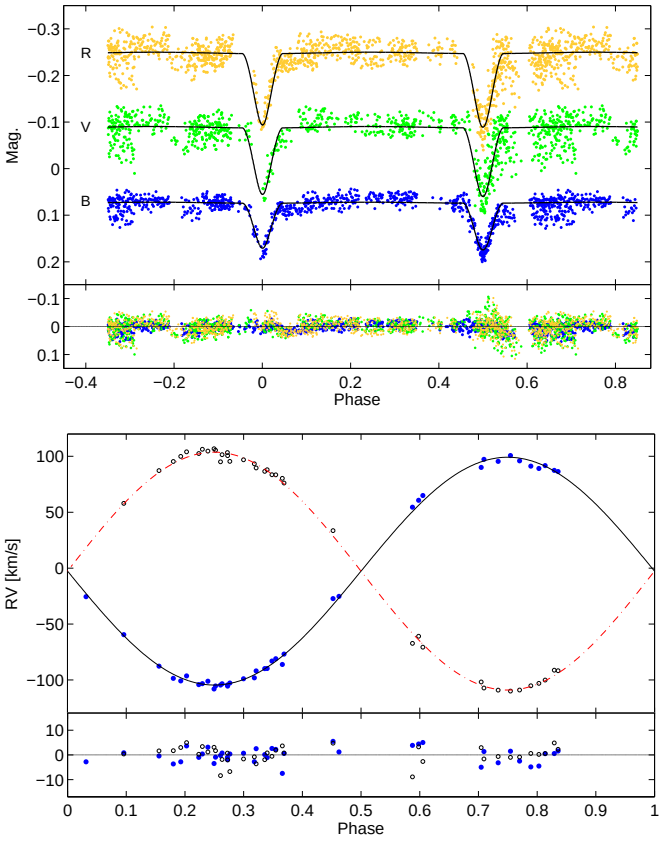

FIG. 7.— Light and radial velocity curve fits of the inner pair of BR Ind based on the PHOEBE fitting.

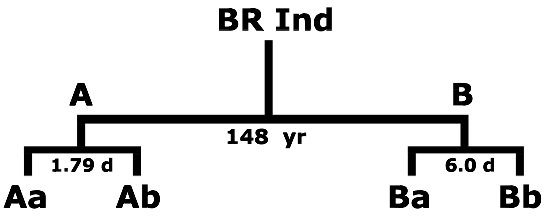

FIG. 8.— Structure of BR Ind as resulted from our analysis.

each other (therefore the problems with 0.89 versus 1.78-days period). Both gamma velocities of the eclipsing pair as well as of the B pair are similar to each other and close to zero. This would indicate that the orbit is very close to face-on orientation, which was confirmed via the fitting of the astrometry (see below). We also collected the available photometry for deriving the times of the eclipses and constructed the $O-C$ diagram plotted in Fig. 9. No visible variation can be seen there during these approximately 25 years of observations. This would also indicate that the period of the visual pair is rather long or the orbit is nearly face-on.

The available positional measurements were analysed leading to slight improvement of the published fit by Seymour et al. (2002). The parameters are given in Table 7 and the plot of the orbit in Fig. 9. As one can see, the period is a bit shorter and the eccentricity higher. The orientation of the orbit is really close to face-on ($i = 155°$), which is in agreement with the discussion in the previous paragraph.

From the fit of the visual orbit we can also derive the total mass of the whole system. This resulted in about

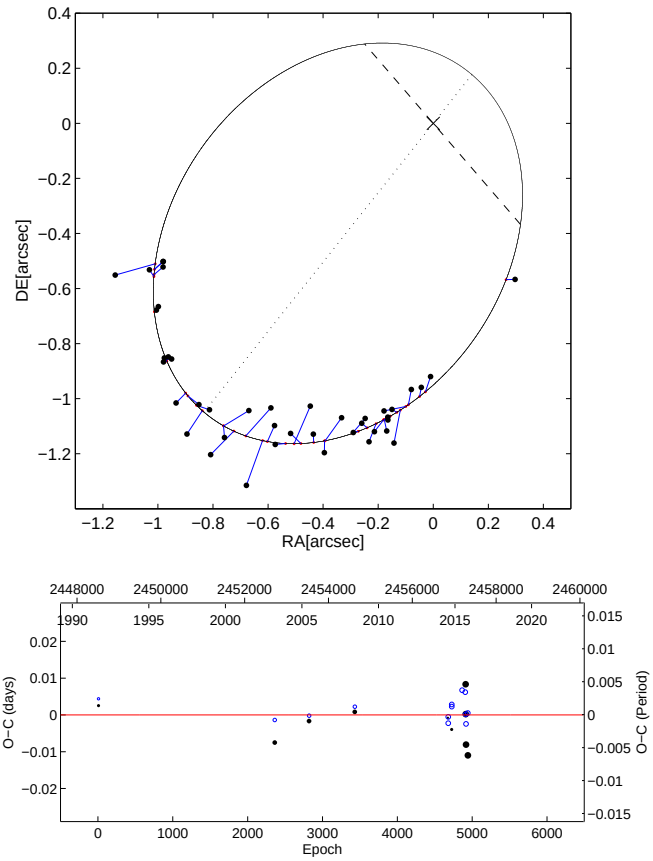

FIG. 9.— Orbit of BR Ind on the sky, and the $O-C$ diagram. See Fig. 2 for description.

TABLE 6
THE PARAMETERS FROM THE LC+RV FITTING OF BR IND.

	Pair A		Pair B
Parameter	Primary	Secondary	
HJD_0	2448500.4755 ± 0.0002		2456563.186 ± 0.052
P [d]	1.7855618 ± 0.0000015		6.0009949 ± 0.0000020
a [$R_\odot$]	7.37 ± 0.04		9.551 ± 0.026
v_γ [km/s]	-2.66 ± 0.08		-3.131 ± 0.089
e	–		0.190 ± 0.003
ω [deg]	–		161.83 ± 0.94
$q = M_2/M_1$	0.96 ± 0.02		–
i [deg]	85.17 ± 1.8		–
K [km/s]	101.9 ± 0.4	106.4 ± 0.4	40.40 ± 0.03
T [K]	5170 (fixed)	5203 ± 75	–
M [$M_\odot$]	0.86 ± 0.02	0.83 ± 0.02	–
R [$R_\odot$]	1.23 ± 0.03	0.95 ± 0.02	–
M_{bol} [mag]	4.78 ± 0.05	5.32 ± 0.06	–
L_B[%]	16.5 ± 2.0	10.2 ± 2.0	73.3 ± 3.5
L_V[%]	24.3 ± 2.3	14.9 ± 1.7	60.8 ± 4.0
L_R[%]	26.3 ± 2.4	16.0 ± 1.6	57.7 ± 4.2

TABLE 7
THE PARAMETERS OF VISUAL ORBIT OF BR IND.

Parameter	Our solution	Seymour et al. (2002)
p_3 [yr]	147.9 ± 2.5	167.0
T_0 [yr]	2050.3 ± 1.9	2056.0
e	0.711 ± 0.021	0.521
a [arcsec]	0.864 ± 0.045	0.894
i [deg]	154.6 ± 8.2	141.9
Ω [deg]	220.8 ± 11.8	142.8
ω [deg]	80.1 ± 9.9	178.4

3.34 $M_\odot$. Such mass can be used to derive the individual masses of the pair B in the system. If we accept the orbital solution as derived from our LC+RV analysis, the mass of the pair B has to be of about 1.65 $M_\odot$. Due to the fact that the B subsystem is only a SB1-type binary, we can only estimate its individual masses. For the SB1-type binary we can calculate a so-called mass function (Kallrath & Milone 2009):

$$f(M)_B = \frac{1}{2\pi G} K^3 P_B \, (1 - e_B^2)^{3/2} = \frac{(M_{Bb} \cdot \sin i_B)^3}{(M_{Ba} + M_{Bb})^2},$$

and from the knowledge of the total mass of pair B we can derive the product $(M_{Bb} \cdot \sin i_B) = 0.47$ $M_\odot$. Obviously, we do not know the inclination of the pair, but at least some estimation can be done also with these values. From the LC solution the third light of the pair B is higher than the combined light coming from the two eclipsing components of pair A. Hence, this finding is in excellent agreement with the masses as derived from the SB1 binary of the pair B and the total mass – but only with the assumption that the inclination is close to 90°. Hence, the two components of the B pair should be of about F8V+M2V. With such a configuration the individual luminosity levels and their ratios as well as the non-detection of the Bb component in the spectra will be explained. Also the spectral classification is now clarified, being of the Ba component instead of the eclipsing pair. And finally, this solution would indicate that the two visual components have their individual magnitudes shifted of about 1.1 mag, which is in agreement with the magnitude differences as published in the WDS catalogue (Mason et al. 2001). However, the whole discussion is solely based on the assumption that the Hipparcos parallax (van Leeuwen 2007) of 20.65 mas is correct.

7. DISCUSSION AND CONCLUSIONS

Regardless of the fact that a lot of work has been done on the theoretical modelling as well as on the observations during the last decades, the formation of systems of higher multiplicity still remains an open question. Multiplicity itself is the most promising mechanism to produce close binaries with short orbital periods below 1 day. A third component may cause Kozai cycles and then the tidal friction between the binary components causes an orbital shrinkage and its circularization, see e.g. Eggleton & Kiseleva-Eggleton (2001) and Borkovits et al. (2016). Nevertheless, this is not the only one possible scenario of origin of such systems and several other competing theories are still being discussed. Truly existing systems were probably produced by a combination of several different mechanisms, see e.g. Tokovinin (2008). The numerical simulations which include only particular mechanisms are able to explain only some statistical properties of the multiple systems, but fail to explain the others. That is a matter of intensive investigation of recent years and each newly discovered multiple system with its known orbital and physical parameters should help us to improve the statistical properties of the sample and provide us with new observational constrains.

The study of three selected eclipsing multiple systems provides us with only a piece of information needed for construction of the theory of stellar formation and evolution. Despite this fact, it is still a valuable contribution to the topic in several aspects. At first, the three systems represent the most typical multiple systems nowadays (containing the close inner pair with the period of a few days and the distant component of much longer period). At second, their physical and orbital properties are now well-determined and can be placed into the broader context of theoretical modelling (e.g. the ratio of periods of the inner and outer orbits, the mass ratios or the eccentricity values), see e.g. Halbwachs et al. (2003) or Tokovinin (2008).

At third, each of the studied systems is somehow interesting and deserves our attention. V773 Cas was found to be much closer to the Sun than originally assumed on the basis of the Hipparcos data. QS Aql is rather massive, but moving around a common barycenter with the third component on the orbit with a very high eccentricity of about 0.95. And also BR Ind was found to be of a rare quadruple system consisting of eclipsing and non-eclipsing pairs. This detection of the higher order multiplicity among the stars of such a late type is also rather remarkable, because for the late type stars their multiplicity fraction is generally very low, see e.g. Duchêne & Kraus (2013). As a common characteristics for all these systems should also be mentioned that in all of them the most massive and most luminous star is the distant third component (apart from BR Ind, where it is a binary). And as was already shown (e.g. by Tokovinin 2008 and Borkovits et al. 2016), such systems are still rather rare.

As a by-product we also derived the possible mutual inclinations for these three systems and their orbits. Due to the fact that longitude of the ascending node of the inner eclipsing pair is not known, we can only estimate the ranges within which the mutual inclination should lie. This resulted in 48–142 deg for V773 Cas, 22–145 deg for QS Aql, and 69–120 deg for BR Ind, respectively. As one can see, the ranges are still rather high and the uncertainty should be lower when knowing the longitude of the ascending node. However, this can only be achieved resolving the inner eclipsing pair via interferometry, which is very problematic (due to the luminous third star and a small angular separation of the eclipsing components). The most promising in this sense seems to be V773 Cas, where the predicted angular distance was computed to be of about 0.8 mas.

And finally, such a study is also viable from the observational point of view. We can see that there still exist many systems never analysed before and their parameters not known, despite the fact that the observations exist and are easily obtainable. At this point it would be suitable to mention that the photometric data for V773 Cas and QS Aql were obtained using only the 34mm-sized telescopes, while BR Ind with a 107-mm one.

We would like to thank the Pierre Auger Collaboration for the use of its facilities. The operation of the robotic telescope FRAM is supported by the EU grant GLORIA (No. 283783 in FP7-Capacities program) and by the grant of the Ministry of Education of the Czech Republic (MSMT-CR LM2015038). The data calibration and analysis related to FRAM telescope is supported by the Ministry of Education of the Czech Republic (MSMT-CR LG15014) and by the Czech Science Foundation

grant No. 14-17501S. The observations obtained with the MPG 2.2m telescope were supported by the Ministry of Education, Youth and Sports project - LG14013 (Tycho Brahe: Supporting Ground-based Astronomical Observations). We would like to thank the observers S. Ehlerová, A. Kawka, P. Kabáth, and S. Vennes for obtaining the data. R. Kříček is also acknowledged for obtaining some of the spectroscopic data. This research has made use of the Washington Double Star Catalog maintained at the U.S. Naval Observatory. This investigation was supported by the Czech Science Foundation grants No. P209/10/0715 and GA15-02112S. We also do thank the ASAS, and Pi of the sky teams for making all of the observations easily public available. This research has made use of the SIMBAD and VIZIER databases, operated at CDS, Strasbourg, France and of NASA's Astrophysics Data System Bibliographic Services.

REFERENCES

Abt, H. A., Gomez, A. E., & Levy, S. G. 1990, ApJS, 74, 551
Bessell, M. S. 1990, PASP, 102, 1181
Borkovits, T., Hajdu, T., Sztakovics, J., et al. 2016, MNRAS, 455, 4136
Burd, A., Cwiok, M., Czyrkowski, H., et al. 2005, New Astronomy, 10, 409
Cannon, A. J., & Pickering, E. C. 1923, AnHar, 98
Cvetković, Z., & Ninković, S. 2010, SerAJ, 180, 71
de Laverny, P., Recio-Blanco, A., Worley, C. C., & Plez, B. 2012, A&A, 544, A126
Docobo, J. A., & Andrade, M. 2006, ApJ, 652, 681
Docobo, J. A., & Ling, J. F. 2007, AJ, 133, 1209
Docobo, J. A., Tamazian, V. S., Andrade, M., Melikian, N. D., & Karapetian, A. A. 2008, AJ, 136, 890
Duchêne, G., & Kraus, A. 2013, ARA&A, 51, 269
Eggleton, P. P., & Kiseleva-Eggleton, L. 2001, ApJ, 562, 1012
Guthnick, P. 1931, AN, 241, 263
Halbwachs, J. L., Mayor, M., Udry, S., & Arenou, F. 2003, A&A, 397, 159
Hartkopf, W. I., & Mason, B. D. 2009, AJ, 138, 813
Heintze, J. R. W., Spronk, W., & Hoekzema, N. 1989, SSRv, 50, 344
Hill, S. N. 1931, PDAO, 6, 11
Holmgren, D. 1987, in BAAS, Vol. 19, BAAS, 709
Horn, J., Kubát, J., Harmanec, P., et al. 1996, A&A, 309, 521
Houk, N. 1978, Michigan catalogue of two-dimensional spectral types for the HD stars
Jaschek, M. 1978, BICDS, 15
Kallrath, J., & Milone, E. F. 2009, Eclipsing Binary Stars: Modeling and Analysis, doi:10.1007/978-1-4419-0699-1
Kazarovets, E. V., Samus, N. N., Durlevich, O. V., et al. 1999, IBVS, 4659
Knipe, G. F. G. 1971, PASP, 83, 352
Lu, L. 1991, PBeiO, 17, 59
Lucy, L. B., & Sweeney, M. A. 1971, AJ, 76, 544
Mason, B. D., Wycoff, G. L., Hartkopf, W. I., Douglass, G. G., & Worley, C. E. 2001, AJ, 122, 3466
Mayer, P. 2004, in ASPC, Vol. 318, Spectroscopically and Spatially Resolving the Components of the Close Binary Stars, ed. R. W. Hilditch, H. Hensberge, & K. Pavlovski, 233–241
Mérand, A., Kervella, P., Pribulla, T., et al. 2011, A&A, 532, A50
Millman, P. M. 1928, PDAO, 4, 97
Nemravová, J., Harmanec, P., Brož, M., et al. 2016, A&A, accepted
Palacios, A., Gebran, M., Josselin, E., et al. 2010, A&A, 516, A13
Palmer, D. R., Walker, E. N., Jones, D. H. P., & Wallis, R. E. 1968, RGOB, 135, 385
Pecaut, M. J., & Mamajek, E. E. 2013, ApJS, 208, 9
Perryman, M. A. C., & ESA. 1997, The HIPPARCOS and TYCHO catalogues (The Hipparcos and Tycho catalogues. Astrometric and photometric star catalogues derived from the ESA Hipparcos Space Astrometry Mission, Publisher: Noordwijk, Netherlands: ESA Publications Division, 1997, Series: ESA SP Series 1200)
Perryman, M. A. C., de Boer, K. S., Gilmore, G., et al. 2001, A&A, 369, 339
Pojmanski, G. 1997, AcA, 47, 467
Prouza, M., Jelínek, M., Kubánek, P., et al. 2010, AdAst, 2010, 849382
Prša, A., & Zwitter, T. 2005, ApJ, 628, 426
Seymour, D. M., Mason, B. D., Hartkopf, W. I., & Wycoff, G. L. 2002, AJ, 123, 1023
Škoda, P. 1996, in ASPC, Vol. 101, Astronomical Data Analysis Software and Systems V, ed. G. H. Jacoby & J. Barnes, 187
Tody, D. 1993, in ASPC, Vol. 52, Astronomical Data Analysis Software and Systems II, ed. R. J. Hanisch, R. J. V. Brissenden, & J. Barnes, 173
Tokovinin, A. 2008, MNRAS, 389, 925
van Hamme, W. 1993, AJ, 106, 2096
van Leeuwen, F. 2007, A&A, 474, 653
Wilson, R. E., & Devinney, E. J. 1971, ApJ, 166, 605
Zasche, P., Uhlař, R., & Svoboda, P. 2014, AcA, 64, 125
Zasche, P., Uhlař, R., Šlechta, M., et al. 2012, A&A, 542, A78
Zasche, P., & Wolf, M. 2007, AN, 328, 928
Zasche, P., Wolf, M., Hartkopf, W. I., et al. 2009, AJ, 138, 664

TABLE 8
List of new minima timings used for the analysis

Star	JD Hel.-2400000	Error [day]	Type	Filter	Source / Observatory
V773 Cas	48500.8874	0.0095	Prim	Hp	Hipparcos
V773 Cas	54798.48508	0.00154	Prim	BVR	PS
V773 Cas	55062.39534	0.00139	Prim	BVR	PS
V773 Cas	55071.45118	0.00133	Prim	BVR	PS
V773 Cas	55410.39017	0.00197	Prim	BVR	PS
V773 Cas	55419.44651	0.00101	Prim	BVR	PS
V773 Cas	55481.54064	0.00182	Prim	BVR	PS
V773 Cas	55754.50689	0.00038	Sec	I	RU
V773 Cas	55776.49780	0.00026	Prim	R	PS
V773 Cas	55776.49748	0.00066	Prim	I	RU
V773 Cas	55877.40172	0.00047	Prim	R	RU
V773 Cas	56155.54350	0.00069	Sec	R	RU
V773 Cas	56159.42162	0.00105	Prim	R	RU
V773 Cas	56230.57514	0.00062	Sec	C	RU
V773 Cas	56252.56717	0.00075	Prim	C	RU
V773 Cas	56304.31383	0.00040	Prim	C	RU
V773 Cas	56516.47530	0.00062	Prim	I	RU
V773 Cas	56538.46837	0.00084	Sec	C	RU
V773 Cas	56851.53476	0.00029	Sec	R	RU
V773 Cas	56930.44650	0.00031	Prim	I	RU
V773 Cas	56978.31353	0.00019	Sec	I	RU
V773 Cas	57199.52681	0.00057	Prim	R	RU
V773 Cas	57234.46016	0.00090	Sec	R	RU
V773 Cas	57348.30130	0.00075	Sec	R	RU
V773 Cas	57383.23313	0.00048	Prim	R	RU
V773 Cas	57569.51959	0.00035	Prim	R	RU
QS Aql	55063.40382	0.00052	Prim	R	PS
QS Aql	55068.43043	0.00350	Prim	BVRI	RU
QS Aql	55068.43052	0.00032	Prim	R	PS
QS Aql	55102.36336	0.00351	Sec	I	RU
QS Aql	55405.20687	0.00170	Prim	BVRI	RU
QS Aql	55480.60724	0.00241	Prim	BVRI	RU
QS Aql	55817.39258	0.00155	Prim	C	RU
QS Aql	56112.70283	0.00113	Sec	R	RU
QS Aql	56113.95940	0.00350	Prim	R	RU
QS Aql	56459.54374	0.01260	Sec	C	RU
QS Aql	56488.44384	0.00122	Prim	C	RU
QS Aql	56870.47101	0.00045	Prim	V	RU
QS Aql	57242.43237	0.00136	Prim	V	RU
QS Aql	57531.46696	0.00212	Prim	V	RU
QS Aql	57580.47669	0.00195	Sec	V	RU
QS Aql	57614.40355	0.00116	Prim	V	RU
BR Ind	48512.97695	0.00227	Prim	Hp	Hipparcos
BR Ind	48513.87160	0.00289	Sec	Hp	Hipparcos
BR Ind	52717.96502	0.00264	Prim	V	ASAS
BR Ind	52718.86393	0.00171	Sec	V	ASAS
BR Ind	53537.54375	0.00136	Prim	V	ASAS
BR Ind	53538.43800	0.00197	Sec	V	ASAS
BR Ind	54628.52452	0.00203	Prim	V	ASAS
BR Ind	54629.41872	0.00287	Sec	V	ASAS
BR Ind	56849.76183	0.00437	Prim	I	FRAM
BR Ind	56857.79538	0.00186	Sec	I	FRAM
BR Ind	56940.82231	0.00777	Prim	I	FRAM
BR Ind	56941.72129	0.02155	Sec	I	FRAM
BR Ind	56857.79712	0.00155	Sec	I	FRAM
BR Ind	56941.72189	0.00119	Sec	I	FRAM
BR Ind	57189.91885	0.00013	Sec	B	FRAM
BR Ind	57264.91192	0.00720	Sec	B	FRAM
BR Ind	57272.94910	0.00060	Prim	B	FRAM
BR Ind	57273.83371	0.00437	Sec	B	FRAM
BR Ind	57274.72655	0.00397	Prim	B	FRAM
BR Ind	57282.75891	0.00281	Sec	B	FRAM
BR Ind	57283.64606	0.00143	Prim	B	FRAM
BR Ind	57325.61535	0.01125	Sec	B	FRAM
BR Ind	57326.49662	0.00326	Prim	B	FRAM

Note: This table is available in its entirety in machine-readable and Virtual Observatory (VO) forms. RU and PS are initials of the co-authors names.

APPENDIX

TABLES OF MINIMA

TABLES OF RADIAL VELOCITIES

TABLE 9
List of the radial velocities used for the analysis.

Star	JD Hel.-2400000	RV_1 [km s^{-1}]	RV_2 [km s^{-1}]	Observatory
V773 Cas	56534.5191	22.964	-6.638	Ond
V773 Cas	56540.5417	-82.834	96.039	Ond
V773 Cas	56563.5964	-85.927	107.335	Ond
V773 Cas	56572.5618	94.114	-81.845	Ond
V773 Cas	56590.3591	43.175	-12.803	Ond
V773 Cas	56596.5316	42.319	-24.662	Ond
V773 Cas	56665.2559	9.844	13.742	Ond
V773 Cas	56666.2016	74.693	-71.150	Ond
V773 Cas	56862.4161	97.931	-83.252	Ond
V773 Cas	56862.5705	99.085	-83.225	Ond
V773 Cas	56924.3821	87.160	-78.330	Ond
V773 Cas	57260.5698	57.533	-50.438	Ond
V773 Cas	57275.4178	-72.467	91.545	Ond
V773 Cas	57284.4024	101.586	-89.144	Ond
V773 Cas	57287.4956	8.957	7.953	Ond
V773 Cas	55497.4625	-71.760	84.909	Ond
V773 Cas	55622.3217	-44.576	59.889	Ond
V773 Cas	55623.3745	93.110	-84.606	Ond
V773 Cas	56192.3778	103.565	-89.690	Ond
V773 Cas	56400.5898	-91.459	92.108	Ond
QS Aql	56013.6415	-47.198	66.622	Ond
QS Aql	56041.5475	-80.691	175.642	Ond
QS Aql	56151.4539	19.518	-107.258	Ond
QS Aql	56192.3915	-91.426	156.803	Ond
QS Aql	56357.6687	-1.965	-64.234	Ond
QS Aql	56400.5732	-42.711	41.075	Ond
QS Aql	56407.5370	55.993	-207.647	Ond
QS Aql	56464.4176	-46.862	61.639	Ond
QS Aql	56527.4023	-12.191	–	Ond
QS Aql	56534.3037	-90.273	172.925	Ond
QS Aql	56534.5020	-83.692	167.165	Ond
QS Aql	56540.2671	32.763	-140.315	Ond
QS Aql	56590.3185	-0.375	-79.928	Ond
QS Aql	56665.1783	-79.765	165.063	Ond
QS Aql	56736.6346	59.747	-223.658	Ond
QS Aql	56772.5975	-45.892	63.491	Ond
QS Aql	56799.4995	57.337	-218.136	Ond
QS Aql	56862.4011	60.692	-204.877	Ond
QS Aql	56924.3353	-43.001	63.641	Ond
QS Aql	57126.5445	32.494	-142.932	Ond
QS Aql	57208.5380	-5.866	–	Ond
QS Aql	57211.3821	39.267	-167.650	Ond
QS Aql	57245.4581	-88.122	169.952	Ond
QS Aql	57260.4073	-77.626	156.522	Ond
QS Aql	57275.3864	-59.986	112.408	Ond
QS Aql	57294.3430	42.652	-156.705	Ond
QS Aql	57323.3276	-79.242	153.787	Ond
QS Aql	57330.2758	4.005	-79.303	Ond
QS Aql	56555.5332	54.385	-217.627	FEROS
QS Aql	56555.5738	58.308	-222.318	FEROS
QS Aql	56555.6103	59.994	-222.843	FEROS
QS Aql	56555.6476	59.324	-231.485	FEROS
QS Aql	56562.5281	-25.677	19.208	FEROS
QS Aql	56562.5807	-16.597	-2.292	FEROS
QS Aql	56563.5079	36.519	-171.487	FEROS
QS Aql	56563.5441	29.523	-163.707	FEROS
QS Aql	56563.6067	25.396	-141.287	FEROS
QS Aql	56564.5231	-89.022	187.011	FEROS
QS Aql	56564.5565	-86.879	189.186	FEROS
QS Aql	56564.5972	-86.505	180.737	FEROS
BR Ind	56555.5550	-103.332	106.265	FEROS
BR Ind	56555.5951	-105.425	105.437	FEROS
BR Ind	56555.6312	-104.541	103.410	FEROS
BR Ind	56555.6801	-98.914	96.941	FEROS
BR Ind	56555.7187	-91.928	89.599	FEROS
BR Ind	56555.7449	-89.879	86.619	FEROS
BR Ind	56555.7783	-81.036	83.418	FEROS
BR Ind	56555.8036	-76.804	76.149	FEROS
BR Ind	56562.5654	-87.647	87.267	FEROS
BR Ind	56562.6090	-98.574	95.403	FEROS
BR Ind	56562.6492	-96.409	104.060	FEROS
BR Ind	56562.6864	-104.150	102.517	FEROS
BR Ind	56562.7140	-101.171	104.689	FEROS
BR Ind	56562.7327	-108.033	106.827	FEROS
BR Ind	56562.7573	-103.429	101.504	FEROS
BR Ind	56563.5972	95.514	-109.126	FEROS
BR Ind	56563.6346	100.678	-109.995	FEROS
BR Ind	56563.6621	95.935	-109.043	FEROS
BR Ind	56563.6965	91.273	-105.220	FEROS
BR Ind	56563.7209	89.127	-102.994	FEROS
BR Ind	56563.7401	91.691	-100.083	FEROS
BR Ind	56563.7676	87.438	-91.302	FEROS
BR Ind	56564.5380	-104.525	95.091	FEROS
BR Ind	56564.5664	-102.728	95.506	FEROS
BR Ind	56564.6411	-98.061	93.281	FEROS
BR Ind	56564.6799	-89.713	87.975	FEROS
BR Ind	56564.7262	-86.142	80.363	FEROS
BR Ind	56986.5334	60.691	-60.939	FEROS
BR Ind	56989.5235	-105.452	100.628	FEROS